# Modeling and Validation of a Multiple Evaporator Refrigeration Cycle for Electric Vehicles

Andreas Varchmin[1]    Manuel Gräber[2]    Jürgen Köhler[1]

[1]Technische Universität Braunschweig, Institut für Thermodynamik *(a.varchmin@tu-bs.de)*
[2]TLK-Thermo GmbH

## Abstract

Multiple evaporator vapor compression cycles become relevant for thermal systems in electric vehicles since batteries and other electric components demand cooling for a secure operation. In difference to most other applications with parallel evaporators cooling demands and temperature levels vary between the different secondary fluids. This leads to a more complex system behavior that needs to be described for optimality and control analysis. In this paper a dynamic model for an automotive air conditioning cycle with an additional evaporator for battery cooling is developed and validated. A battery model library for calculating temperatures and waste heat flows of battery cells and modules is presented. Multi-evaporator effects and their consequences are discussed. Reasonable actuating and control variables are chosen and a discussion regarding possible control schemes is given.

*Keywords: Multi-Evaporator Cycle, Parallel Evaporators, Vapor Compression Cycle, Electric Vehicle, Relative Gain Array*

## 1 Introduction

Battery electric vehicles (BEV) or plug-in hybrid electric vehicles (PHEV) require a more complex thermal system and vapor compression cycle than conventional vehicles. In many cases heat needs to be gained, respectively led away, at more than one spot. One important spot is the battery that needs to be in a reasonable and safe temperature zone. Depending on the ambient conditions the heat gathered at the battery or the power electronics can be used for operating a heat pump.

For maximum lifetime battery temperatures should lie between 15°C and 35°C and show small temperature gradients over battery cells and modules (Pesaran et al., 2013). Maintaining these temperatures leads to the necessity of active battery cooling. The most common way of active cooling are cooling plates under or between battery cells. These plates are flown through with a cooling liquid like a water-glycol-mixture but can also be used to directly evaporate a refrigerant. Based on a typical air-conditioning unit that owns an evaporator for air cooling a second evaporator is needed to cool battery and possibly power electronics, too.

A heat pump might be necessary for heating the cabin at low temperatures. In conventional vehicles heat from the engine's exhaust is used for heating. In BEVs the battery is the only source of energy which is, due to energy densities of current batteries, small compared to conventional vehicles. A regular electric heater would heavily shorten the vehicle's range. Therefore switchable vapor compression cycles that can function as air conditioning or heat pump have been designed (Ahn et al., 2015). When operating as heat pump the cycle might gain heat from the ambient but also, if available, from battery, electric motor or power electronics. In this case a second evaporator is also necessary.

Multiple evaporator vapor compression cycles are known in different applications. In supermarket refrigeration cycles a high number of evaporators are connected in parallel so that every cabinet can be cooled independently. Mostly thermostatic expansion valves are used to regulate the fluid flow in every cabinet. Furthermore there are systems with more than one compressor unit to create two pressure levels for refrigerators and freeze cabinets. These two pressure levels are connected in parallel as well (Titze et al., 2013). Another multi-evaporator application are HVAC systems in buildings. Especially in commercial buildings so called variable refrigerant flow systems are increasingly used with multiple evaporators for locally distributed cooling zones (Elliott et al., 2011). Usually parallel evaporators are used in these applications. Vapor Compression Cycles with serial connected evaporators exist in fewer applications, e.g. in simple fridge freezers.

In contrast to the described systems the operation of vapor compression cycles in vehicles is a lot more transient. Furthermore the temperatures of the different secondary fluids can be apart whereas temperatures in supermarket cabinets, respectively cooling zones in buildings, share a nearly identical temperature. Since the thermal system needs to be as compact as possible, only one pressure level for both evaporators is practicable (see fig-

ure 1). This makes the optimal operating point less evident and leads to advanced control schemes. Modeling approaches for automotive air conditioning cycles in Modelica with particular attention to evaporators have been published by Limperich et al. (Limperich et al., 2005).

For a better understanding and for fast controller design a simulation model for an automotive multi-evaporator system is developed in this paper. It is concentrated on battery and cabin cooling instead of heat pump operation in electric vehicles. Measurement data obtained from a test bench is used for validation of the model and the system is analyzed for a suitable controller design. Fundamental effects and interdependencies of the evaporators are shown. Gained knowledge is then used to control the multi-evaporator system under conditions of a transient real-life driving cycle.

### Structure of the Paper

In section 2 a model of an automotive air conditioning system with parallel evaporators for cabin and battery cooling is described. In section 3 follows a description of an electric-thermal model of a lithium-ion battery for calculating temperatures and heat flows of cells and modules. An overview of a test bench containing three plate heat exchangers is given in section 4. All secondary fluids in this system are liquids since measurement data can be obtained easily and fast for this configuration. Section 5 shows the interaction of actuating and control variables as superheats or cooling capacities. Moreover the parallel evaporator model is validated with measurement data. Section 6 analyzes the interdependencies of actuating and control variables. With the help of relative gain arrays (RGA) possible controller schemes are discussed. In section 7 simulation results for the parallel evaporator system are shown. Section 8 summarizes the paper and proposes possibilities for future work.

## 2 Automotive Air Conditioning System with Additional Evaporator for Battery Cooling

In the following a dynamic model of a parallel evaporator vapor compression cycle for electric vehicles including battery cooling is described, see figure 1. A description of the implied control scheme is given in section 6. The system has two parallel paths on the low pressure side and consists of a compressor, three heat exchangers, two electronic expansion valves (EXV) and a receiver. As refrigerant R134a is used. The compressor is a variable speed scroll compressor. The receiver is located on the high pressure level behind the condenser so that there is zero subcooling in mostly all operating points since the receiver separates gas from the liquid. This does not lead

to the most efficient behavior because small degrees of subcooling normally have a positive impact on the coefficient of performance (COP). The condenser is a multi port extruded tube (MPET) heat exchanger, situated at the vehicle's front end. Ambient air is used as the condenser's secondary fluid, leading the heat out of the cycle. In modern cars often condensers with an integrated receiver and an additional subcooling zone are used for optimal COPs. Behind the receiver the refrigerant path is divided and leads to an EXV each. In the first path there is located one MPET heat exchanger for cooling the cabin air. In the parallel path a plate heat exchanger is used for cooling the battery. Due to evaporating temperatures falling occasionally under $0°C$ a 50/50 mixture of water and glycol flows through the secondary path of this evaporator. Nearly all model approaches are based on the model library *TIL* (see Richter (2008)). Physical properties are calculated with *TILMedia* (see Schulze (2013)).
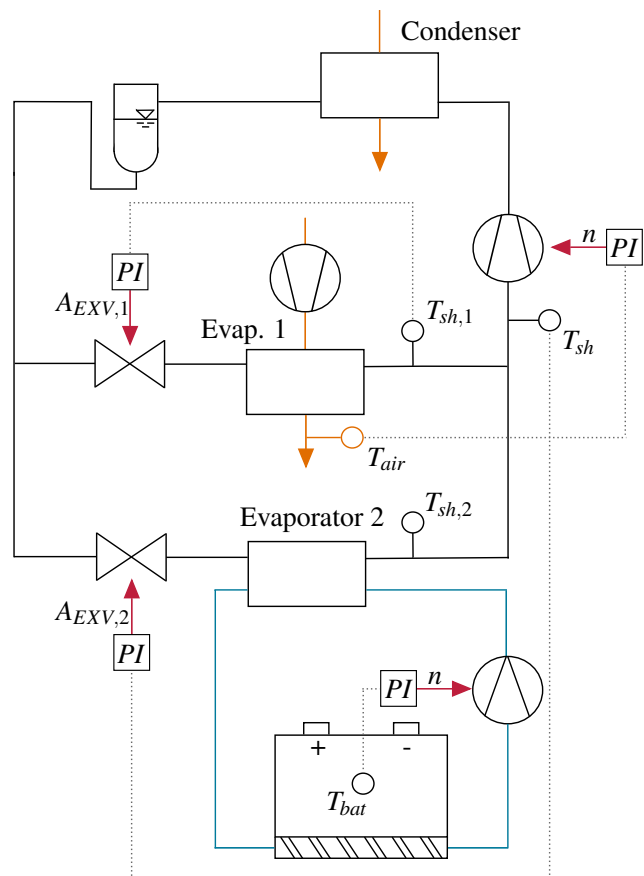


**Figure 1.** Vapor Compression Cycle for a Battery Electric Vehicle including Battery Cooling

The compressor is modelled dynamically with a loss-based approach, including leakage and friction losses (Schedel et al., 2013). The model is fitted to the compressor found in the test bench described in section 5. The EXV model is based on Bernoulli's principle and is therefore a static model. For modelling the heat exchangers a finite volume approach with a variable number of

volumes is used. One volume is described by three cells for refrigerant, liquid and wall material. The liquid and air cells contain transient balances for mass and energy, the refrigerant cell additionally owns a momentum balance. The pressure time derivative is constant over all refrigerant cells of one pressure level. This can be interpreted as a neglection of sonic effects which is appropriate for systems that are not characterized by fast dynamics (Gräber et al., 2010). The receiver model owns one volume with a transient mass and energy balance and has a varying filling level.

The valve openings $A_{EXV,1}$, $A_{EXV,2}$ and the compressor speed $n$ are actuating variables of the primary (refrigeration) cycle. Typical control variables would be the two superheats $T_{sh,i}$, the first evaporator's air outflow temperature $T_{air}$ and the battery temperature $T_{bat}$. Alternatively the cooling capacities $\dot{Q}_i$ of both evaporators could be used. Referring to section 6 it becomes apparent that in difference to a standard refrigeration cycle the numbers of actuating variables and control variables of the primary cycle are not equal.

## 3   Battery Model

To integrally describe thermal systems of electric vehicles as the one discussed in this paper, the behavior of the battery needs to be represented. Important approaches and equations are published in the Modelica Energy Storage Library (Einhorn et al., 2011). For a good suitability and usability regarding automotive systems an electric-thermal battery model library has been developed. The library is designed as an add-on to the component library *TIL* and provides models for battery cells, modules and systems. It is focused on describing temperatures, waste heats and cooling approaches.

In the library battery systems can be discretized down to cell level. Cells can be connected in series or parallel. Each discretization element owns a state of charge (SOC), an electric equivalent circuit, a dynamic energy balance and calculates arising heat flows. The state of charge is coupled with the open circuit voltage. The equivalent circuit can be switched between a model with a single ohmic resistance and an impedance based model. Heat results from different processes inside the battery cells. Losses can be divided in irreversible and reversible heat flows:

$$\dot{Q}_{irr} = -I^2 R_i \tag{1}$$

$$\dot{Q}_{rev} = T \Delta S \frac{I}{nF} \tag{2}$$

The irreversible heat is dependent from the electric current, that is defined by the power demand of the motor and from the impedance which itself is dependent from cell temperature and SOC. The reversible heat is dependent from entropy differences that occur at the electrodes, e.g. because of lithium intercalations in lithium-ion cells. The equation is only exact for isothermal processes but may also be used when temperature changes. $\Delta S$ is the molar entropy change while $n$ represents the number of electrons per reaction and $F$ the Faraday constant. These differences are cell dependent and are functions of the SOC. This approach is described extensively by Viswanathan et al. (Viswanathan et al., 2009). They have also published data for various cell types in the same paper.

The model used in the automotive system described in the previous section is adapted to a battery system in a BEV with 300 prismatic lithium-ion cells. The modules are chilled by cooling plates underneath and contain twelve cells each, at which each three cells are connected in parallel. Water-glycol is used as cooling liquid.
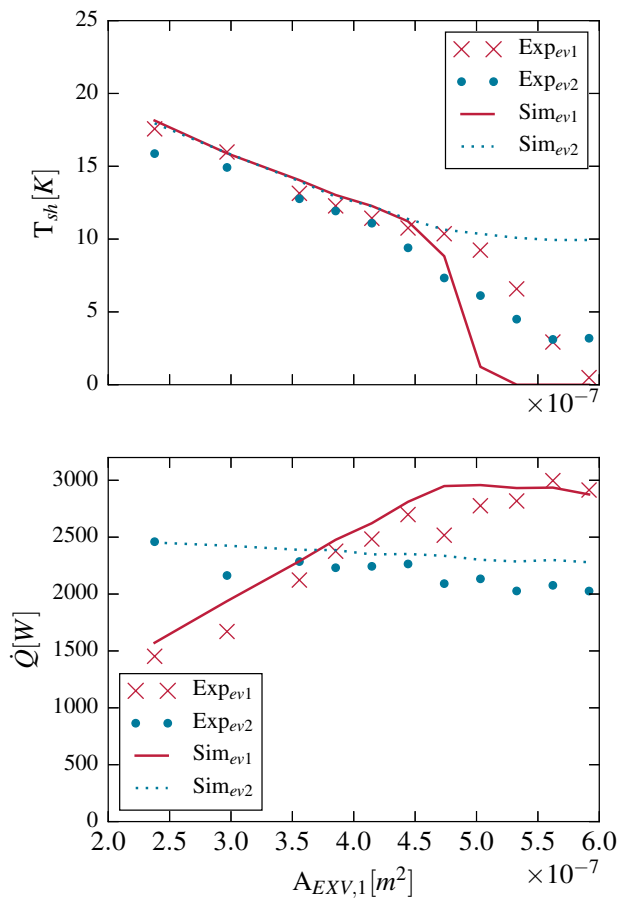
## 4   Test Bench

The test bench contains a refrigeration cycle similar to the one described in section 2. It is dimensioned to fit an automotive air conditioning and cooling application. One difference is that all three heat exchangers are plate heat exchangers receiving and giving off heat by secondary loop cycles filled with water (condenser) or respectively water-glycol mixture (evaporators) as shown in figure 2. This originates from easier and more accurate measuring when handling liquids instead of gases. Both evaporators have same dimension and are of the same type. Another difference to the system model is that a battery is not included since it is focused on the multiple evaporator behavior. Anyway the inflow liquid temperatures of the evaporators $T_{liq,1}$ and $T_{liq,2}$ can be manipulated by electric heaters. Furthermore the mass flow rates $\dot{m}_{liq,1}$ and $\dot{m}_{liq,2}$ are controlled as well.

The scroll compressor works with direct current and variable speed. The EXV is driven by a stepper motor with constant adjusting speed. At various positions temperatures and pressures are measured. The refrigerant mass flow rate is measured behind the compressor in the pure gas zone. The primary cycle of the test bench is pictured in figure 3.

All temperatures are measured with thermocouples. The liquid mass flow rates are measured with magnetic flow meters while the refrigerant mass flow rate behind the compressor is measured by coriolis principle. This means that the cooling capacitiy measuring of the evaporators are based on the liquid side when both evaporators are in use. The quality of stationary measurements can be controlled with the help of results that are gathered by only one evaporator operating. In this case one cooling capacity can be obtained based on the refrigerant side using the more accurate coriolis flow meter and compared to the measurements based on the liquid side.

**Figure 2.** Parallel Evaporator Cycle with Liquids in the Secondary Cycles Existing in the Test Bench



**Figure 3.** Test Bench with Compressor, Receiver, Both Evaporators, Condenser and Expansion Valves



**Figure 4.** Superheats and Cooling Capacities of both Evaporators Depending on Compressor Speed at Different Valve Openings

# 5 Interdependencies and Validation

In this section interdependencies of the two evaporators and the reaction of control variables to actuator changes are shown to visualize multiple evaporator system effects. This is accompanied by a comparison between simulation and measurement results. Simulation results are provided by a model of the test bench that uses the same modeling principles as the overall system model described in section 2.

Since both evaporators in the test bench are equal the cycle will behave like a vapor compression cycle with only one evaporator if all boundary conditions and the valve openings are equal. Hence, in the following one evaporator boundary condition or one valve actuator differs from the other and stationary results are compared. All control loops are open in these experiments.

In figure 4 the superheats and cooling capacities of both evaporators over compressor speed are shown. The valve opening of $EXV_1$ is around 65% higher than the one of $EXV_2$. Both superheats rise with rising speed since the low pressures falls with higher speed and the dew line of R134a has an ascending slope at all relevant operating points. As expected the cooling capacities rise with rising compression power. The effect on evaporator 1 seems higher than the effect on evaporator 2 for both control variables. The overall cooling capacity does not rise as much as one could have expected since in a lot of applications capacity is controlled by compressor speed. At lower speeds superheat 1 is smaller as superheat 2 because of a higher mass flow rate in path 1. Anyway it rises faster and equals superheat 2 at higher compressor speeds. When looking at further (not displayed) results it can be seen that both superheats reach a maximum that is defined by the temperatures of the inflowing secondary liquids minus the evaporating temperature. This maximum superheat is equal for both evaporators since they share the same low pressure and inlet state. Measurement and simulation results of the superheats match very well with a maximum deviation of 2.9 K. Results of evaporator 2 cooling capacity match

very well with a maximum deviation of 160 W. Results for capacity 1 vary up to 365 W.



**Figure 5.** Superheats and Cooling Capacities of both Evaporators Depending on Valve Opening $A_{EXV,1}$ with Constant Valve Opening $A_{EXV,2} = 3.7 \cdot 10^{-7} m^2$

Figure 5 also shows superheats and cooling capacities. The compressor speed and the valve opening area $A_{EXV,2} = 3.7 \cdot 10^{-7} m^2$ are set constant but $A_{EXV,1}$ is varied. At low opening areas the superheats again reach a maximum value of the superheat. Anyway both superheats drop because of a rising low pressure. At $A_{EXV,1} = 4.5 \cdot 10^{-7} m^2$ the simulated superheat 1 starts to fall faster, the measured superheat 1 starts falling faster at $5.0 \cdot 10^{-7} m^2$. Both reach zero superheat with nearly the same opening difference. The measured values of superheat 2 fall as well (to 3 K) while the simulations state that values still reach maximum superheat. The first evaporator's cooling capacity rises with higher openings of its corresponding valve. The second evaporator's capacity falls slightly since mass flow rates through the second path drop. Apart from one measurement point at $A_{EXV,1} = 4.7 \cdot 10^{-7} m^2$ which may be due to a non-stationary operation while measuring, simulation results of the capacities fit to measurement data very well. Summarizing it can be stated that a valve opening area influences the evaporator in its own path more than the other

one and that superheats share the same trend while cooling capacities go in different directions.
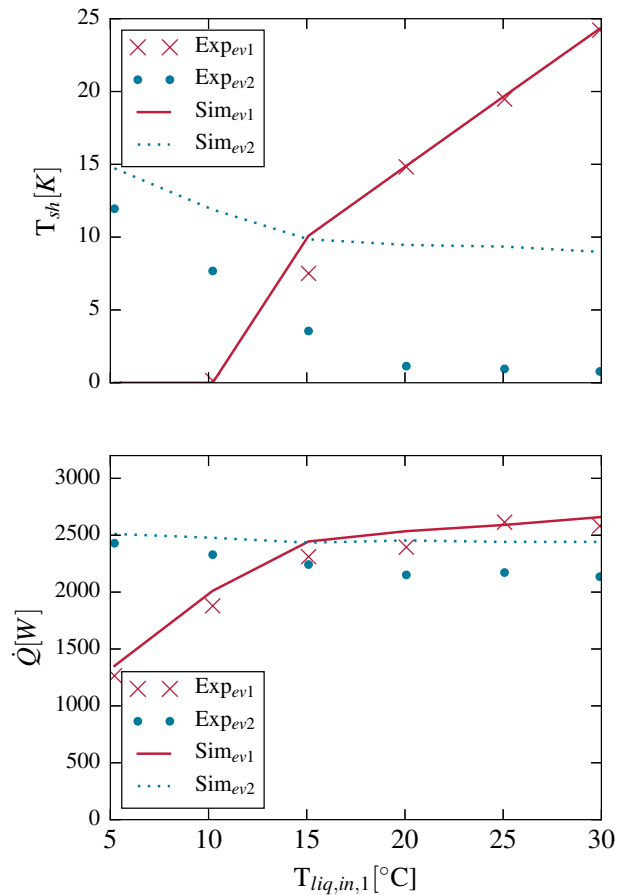


**Figure 6.** Changing of Superheats and Cooling Capacities with Varying Liquid inflow Temperature $T_{liq,in,1}$

The investigation shown in figure 6 deals with a changing boundary condition, precisely the secondary fluid inflow temperature of evaporator 1. The temperature changes from 5°C to 30°C while the temperature of the second liquid stays constant at 15°C. Deviant secondary fluid temperatures of more than a few Kelvins would not be typical for building or supermarket applications but occur in vehicles, e.g. if the cabin is already cooled down while battery and power electronics produce a lot of waste energy. In fact in many cases it will be more efficient to operate the battery at temperatures up to 35°C, needing smaller cooling capacities, while the cabin temperature is controlled to around 20°C. It can be seen that superheat 1 rises with rising temperature as one could have expected. Superheat 2 drops because the low pressure level is lifted with higher evaporating temperatures. The same behaviors are observed for cooling capacities. The evaporator with higher secondary fluid temperature transports more heat. The overall heat capacity reaches a maximum at same secondary fluid temperatures, meaning also a maximum efficiency. Simulation results of evaporator 1 fit very well to measurement data while the reaction to deviant

temperatures is not optimal at evaporator 2. It needs to be considered that small deviations of the exchanged heat lead to high deviations in superheat. Only a small part of the heat is used for superheating while most of it vaporates the refrigerant.

Some of the occuring main effects can be summarized:

- The Compressor speed influences both evaporators but has more effect on the evaporator with higher cooling capacity. It nearly has no effect on the lower cooling capacity.

- Changes in EXV opening areas lead both superheats in the same direction while cooling capacities move in opposite directions. EXVs has a higher influence on the evaporator in its corresponding path.

- Different secondary fluid temperatures lead to different cooling capacities. Control variables shift to opposite directions when one temperature is changed.

With regard to the validation results it can be stated that the occurring effects are represented in the parallel evaporator model, also the ones that may not be clearly self-explanatory. In further work more investigations have been done with deviant actuator variables and boundary conditions that also lead to interesting effects. Deviations between simulation and experiment data are similar to the ones shown here.

## 6  System Analysis

The previous sections shows effects of a multi-evaporator system that need to be analyzed systematically. With the help of the validated model the interdependencies can be quantified.

A good overview of design and operation of a vapor compression cycle with a single evaporator is given by Jensen and Skogestad (2007). They state that a simple vapor compression cycle is optimally designed if there is no superheating and a small degree of subcooling. To reach zero superheating, which means an optimal heat transfer in the evaporator, a low-pressure receiver can be used in simple cycles. In a multiple evaporator cycle a low-pressure receiver would ensure a secure operation of the compressor but not lead automatically to an optimal operation point. An overall superheat of zero does not mean zero superheat in each of the evaporators. It will be more likely that the outflow refrigerant of one evaporator has a high degree of superheat while the other evaporator's outflow state lies inside the two-phase region. Both superheats need to be controlled and the advantage of a low-pressure receiver disappears. In automotive air conditioning systems reaching a small degree of subcooling is often done by a condenser unit with integrated receiver and a short subcooling zone. This paper concentrates on

evaporators so that for an easier test bench setup there is no subcooling zone behind the high-pressure tank (see figure 2).

From an operation view the compressor work (here speed) and the valve openings can be manipulated. The active refrigerant mass is adjusted by the receiver. Since both superheats need to be controlled and it is desirable to control both cooling capacities (or the outflow temperatures $T_{liq,1}$) one actuating variable is missing to regulate all four control variables independently. In many multi-evaporator systems, e.g. in the ones mentioned in the introduction, the cooling capacities do not need to be controlled seperately because the temperature setpoints of the different secondary fluids are equal. In the case of similar thermal load the control variables can be controlled together.

One obvious way to control the cooling capacities seperately is manipulating a secondary fluid mass flow rate $\dot{m}_{liq}$ (e.g. through pump speed). The mass flow changes the effective heat transfer in the corresponding evaporator. This leads to an optimization problem between pump work and primary cycle's efficiency. Moreover the mass flow rates are often given by other conditions. In the system analysed here manipulating the battery cooling liquid mass flow rate seems to make sense.

The described interdependencies between the control variables demand special controller designs. Reasonable approaches could be a decoupling control that prevents change in other process variables when one variable is changed or a dynamic feedforward control that has knowledge about the physical behavior as described in previous work (Varchmin et al., 2014). However development of advanced control schemes is not the main focus of this paper. Hence, Single-Input-Single-Output (SISO) controllers are used for the automotive system described in section 2, even if a decoupling seems to be recommended as it is shown in the following.

| $n = 3000 rpm$ | $n$ | $A_{EXV,1}$ | $A_{EXV,2}$ | $\dot{m}_{liq,2}$ |
|---|---|---|---|---|
| $\dot{Q}_1$ | 0.38 | **0.56** | 0.05 | 0.01 |
| $\dot{Q}_2$ | 0.33 | 0.04 | **0.61** | 0.02 |
| $T_{sh}$ | 0.05 | 0.03 | 0.4 | **0.52** |
| $T_{sh,1}$ | **0.24** | 0.36 | -0.06 | 0.45 |

| $n = 6000 rpm$ | $n$ | $A_{EXV,1}$ | $A_{EXV,2}$ | $\dot{m}_{liq,2}$ |
|---|---|---|---|---|
| $\dot{Q}_1$ | **0.66** | 0.14 | 0.07 | 0.12 |
| $\dot{Q}_2$ | 0.33 | 0.02 | 0.32 | **0.32** |
| $T_{sh}$ | -0.12 | -0.06 | **0.81** | 0.38 |
| $T_{sh,1}$ | 0.13 | **0.9** | -0.2 | 0.17 |

**Table 1.** Relative Gain Arrays of Two Evaporator System at Different Compressor Speeds

For Multi-Input-Multi-Output (MIMO) systems steady-state interactions, e.g the ones shown in the previous section, can be represented in relative gain arrays (RGA). These matrices show normalized steady-state gain information and are therefore a measure of interactions (Grosdidier et al., 1985). In table 1 two RGAs derived by the validated model are shown. RGAs quantify system behavior and may be used to develop SISO (as well as MIMO) controller schemes, i.e. to obtain reasonable pairs of actuating and control variables (Skogestad and Postlethwaite, 2007). The arrays are different for every operation point, only for a linear system one array would be valid globally. Gain scheduling could be used to adapt controller parameters to nonlinear behavior in dependence of the current operating point.

The displayed arrays are valid for two different compressor speeds, i.e. cooling capacities, at small superheats. Instead of the superheat of evaporator 2 the overall superheat in front of the compressor is chosen as a control variable. Firstly the overall superheat is most relevant for a secure compressor operation and secondly the RGAs are less coupled in this case. Optimal actuator-control pairs for the operation points are printed in bold. It can be seen that the system is highly nonlinear and that actuating variables that are a good choice in one point may be a useless choice in another. While the reactions to changes of compressor speed $n$ stay similar (first column) the reactions of the other actuating variables differ a lot. E.g. the mass flow rate $\dot{m}_{liq}$ would be best paired with cooling capacity $\dot{Q}_1$ for $n = 6000 rpm$ (value 0.32) bus has nearly no effect for $n = 3000 rpm$ (0.02).

The RGAs do not give any information about the system dynamics. Similar time constants complicate SISO control and may lead to instabilities. This may be due to two controllers having influence on the same control variables that wind up to not desired behavior because they disturb each other simultaneously. This problem will be discussed in combination with advanced controller designs in future work.

# 7 Simulation Results

System analysis leads to a control scheme for the automotive system that is shown in figure 1. Four SISO Controllers implemented as PI controllers are used for reaching reasonable setpoints. As discussed table 1 shows possible pairs of actuating and control variables. Values change for different compressor speeds and so a compromise between the operation points needs to be found. Speed $n$ and opening area $A_{EXV,1}$ can be chosen without issues for $\dot{Q}_1$ and $T_{sh,1}$ because of high values in both matrices. It seems best to choose opening area $A_{EXV,2}$ for $\dot{Q}_2$ and the liquid mass flow rate $\dot{m}_{liq,2}$ for the overall superheat $T_{sh}$ because of satisfying values for these pairs in both matrices. A problem for this configuration is that

in some operating points the battery would not be able to provide enough heat to ensure a sufficient superheat. The secondary liquid cycle would need to be designed for very high heat flows that do not occur very often. Therefore the controller scheme of the lower matrice in table 1 is chosen although the dependency between $\dot{m}_{liq,2}$ and $\dot{Q}_2$ is not very strong for slow compressor speeds. It may be a benefit that at high battery temperatures the compressor speed will probably lie over 3000 rpm so that there would be a sufficient coupling again.

The model is simulated with a transient real-life driving cycle (leading from Braunschweig to Wolfsburg) as a boundary condition (see figure 7). The ambient temperature is 30°C and all components possess this temperature at the start of the simulation. The air flowing into the cabin has a temperature of 10°C and the setpoint for the superheats is 7K. For the battery temperature controller a setpoint of 30°C is chosen whereat it is considered that this point will not be reached at all times. The inner battery temperature has a high time constant since the battery owns a great heat capacity and the heat needs to be conducted through the cell until it is led away by the liquid cycle. Only by predictive control it could be controlled perfectly.

Results are shown in figure 7 (b)-(f). At the beginning of the cycle the compressor speed is high to cool down the air and evaporator masses (c). After about one minute the compressor slows down to approximately 3000 rpm. The temperature of the inflowing air reaches its setpoint of 10°C quite fast and remains at this level for the whole cycle (d). The battery temperature rises slowly until around 800 s (f). From that time on the driving cycle reaches higher velocitys and drive power rises. This leads to a faster rising battery temperature. Hence, the cooling liquid mass flow rate is set higher (b). This shows effect at about 800 s so that the battery temperature slope is eased and in the following negative. As discussed previously the main target of battery cooling is not reaching a certain setpoint but limiting the maximum temperature to 35°C. Superheats stay in a secure range except for a small peak at 50 seconds. The overall superheat rises between 200 and 1000 seconds (e). The EXV in the battery cooling path reacts to this deviation (not displayed) but can not balance perfectly since the mass flow rate of the battery cooling liquid is also rising until 1000 seconds.

# 8 Conclusion

In this paper a dynamic model for an air conditioning cycle with an extra evaporator for battery cooling has been developed. A library with physical models for battery cells and modules has been described. Multi-evaporator effects were shown and explained. The developed cycle model has been validated with the help of a test bench containing plate heat exchangers. Elaborated intedepen-
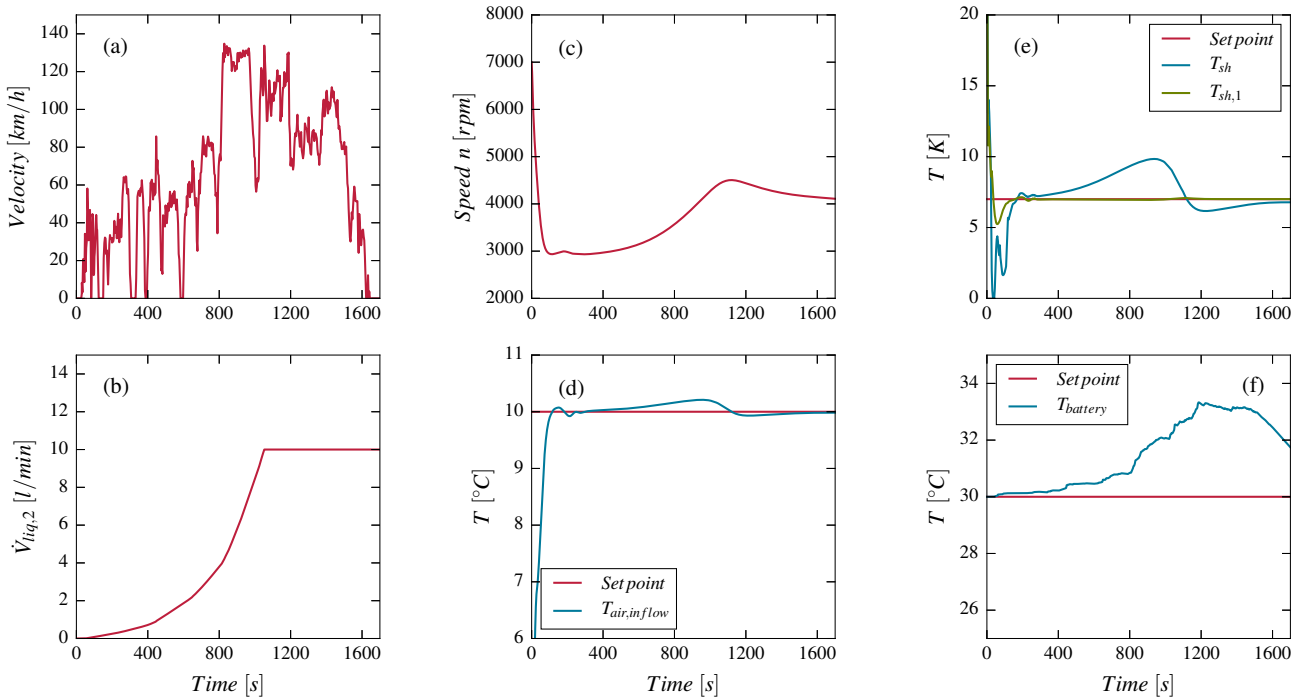
**Figure 7.** Simulation Results of the Automotive System due to a Driving Cycle

dencies were examplewise quantified by relative gain arrays. One of the results is that in difference to a standard vapor compression cycle only three actuating variables of the primary cycle exist for four control variables. This leads to an optimization problem instead of simple optimality conditions. Based on this analysis a SISO controller scheme was derived and simulation results were presented. With the developed model different battery types and cooling approaches can be tested. Furthermore advanced control schemes can be tested and a system efficiency analysis can be performed.

Future work will deal with analysis of multi-evaporator system dynamics and the arising optimization problem. Moreover advanced multivariable controller designs could be developed for an optimal and secure operation.

# Acknowledgements

# References

J.H. Ahn, H. Kang, H.S. Lee, and Y. Kim. Performance characteristics of a dual-evaporator heat pump system for effective dehumidifying and heating of a cabin in electric vehicles. *Applied Energy*, 146:29–37, 2015. doi:10.1016/j.apenergy.2015.01.124.

M. Einhorn, F.V. Conte, C. Kral, C. Niklas, H. Popp, and J. Fleig. A modelica library for simulation of elecric energy storages. *8th International Modelica Conference, Dresden, Germany*, 2011.

M.S. Elliott, C. Estrada, and B.P. Rasmussen. Cascaded superheat control with a multiple evaporator refrigeration system. *American Control Conference, San Francisco, USA*, 2011.

M. Gräber, K. Kosowski, C. Richter, and W. Tegethoff. Modelling of heat pumps with an object-oriented model library for thermodynamic systems. *Mathematical and Computer Modelling of Dynamical Systems*, 16:195–209, 2010. doi:10.1080/13873954.2010.506799.

P. Grosdidier, M. Morari, and B.R. Holt. Closed-loop properties from steady-state gain information. *Industrial and Engineering Chemistry Fundamentals*, 24:221–235, 1985. doi:10.1021/i100018a015.

J.B. Jensen and S. Skogestad. Optimal operation of simple refrigeration cycles. part i: Degrees of freedom and optimality of sub-cooling. *Computers and Chemical Engineering*, 31: 712–721, 2007. doi:10.1016/j.compchemeng.2006.12.003.

D. Limperich, M. Braun, and G. Schmitz. System simulation of automotive refrigeration cycles. *4th International Modelica Conference, Hamburg, Germany*, 2005.

A.A. Pesaran, M. Keyser, K. Smith, G.H. Kim, and S. Santhanagopalan. Tools for designing thermal management of batteries in electric drive vehicles. *Large Lithium Ion Battery Technology & Application Symposia Advanced Automotive Battery Conference, Pasadena, USA*, 2013.

C. Richter. *Proposal of New Object-Oriented Equation-Based Model Libraries for Thermodynamic Systems*. PhD thesis, Technische Universität Braunschweig, 2008.

F. Schedel, G. Suck, S. Försterling, W. Tegethoff, and J. Köhler. Effizienzbewertung von wärmepumpen in hybrid-fahrzeugen mit hilfe der verlustbasierten modellierung von scrollverdichtern. *DKV-Tagung, Hannover, Germany*, 2013.

C. Schulze. *A Contribution to Numerically Efficient Modelling of Thermodynamic Systems*. PhD thesis, Technische Universität Braunschweig, 2013.

S. Skogestad and I. Postlethwaite. *Multivariable Feedback Control: Analysis and Design*. Wiley, 2007.

M. Titze, N. Lemke, A. Hafner, and J. Köhler. Entwicklung und simulation luftaufbereitungs- und kälteanlageanlage im supermarkt mit wärmerückgewinnung. *DKV-Tagung, Hannover, Germany*, 2013.

A. Varchmin, M. Gräber, W. Tegethoff, and J. Köhler. Superheat control with a dynamic inverse model. *10th International Modelica Conference, Lund, Sweden*, 2014.

V.V. Viswanathan, D. Choi, D. Wang, W. Xu, S. Towne, R. Williford, J.-G. Zhang, J. Liu, and Z. Yang. Effect of entropy change of lithium intercalation in cathodes and anodes on li-ion battery thermal management. *Journal of Power Sources*, 195:3720–3729, 2009. doi:10.1016/j.jpowsour.2009.11.103.